NJC

Accepted Manuscript

Volume 40 | Number 1 | January 2016 | Pages 1–846

NJC

New Journal of Chemistry
www.rsc.org/njc

A journal for new directions in chemistry

ISSN 1144-0546

ROYAL SOCIETY
OF CHEMISTRY

PAPER
Jason B. Benedict et al
The role of atropisomers on the photo-reactivity and fatigue of
diarylethene-based metal–organic frameworks

cnrs

This is an Accepted Manuscript, which has been through the Royal Society of Chemistry peer review process and has been accepted for publication.

Accepted Manuscripts are published online shortly after acceptance, before technical editing, formatting and proof reading. Using this free service, authors can make their results available to the community, in citable form, before we publish the edited article. We will replace this Accepted Manuscript with the edited and formatted Advance Article as soon as it is available.

You can find more information about Accepted Manuscripts in the author guidelines.

Please note that technical editing may introduce minor changes to the text and/or graphics, which may alter content. The journal's standard Terms & Conditions and the ethical guidelines, outlined in our author and reviewer resource centre, still apply. In no event shall the Royal Society of Chemistry be held responsible for any errors or omissions in this Accepted Manuscript or any consequences arising from the use of any information it contains.

ROYAL SOCIETY
OF CHEMISTRY

rsc.li/njc

Journal Name

ARTICLE

Fluorous molecules for dye-senzitized solar cells: synthesis and properties of di-branched, di-anchoring organic sensitizers containing fluorene subunits

Ilir Pecnikaj,[a] Daniela Minudri,[b] Luis Otero,[b] Fernando Fungo,*[b] Marco Cavazzini,[c] Simonetta Orlandi[c] and Gianluca Pozzi*[c]

Four organic sensitizers having a di-branched molecular structure D-(π-A)₂ (D = para-substituted arylamine, π = 9,9-dibutylfluorene, A = cyanoacrylic acid) were synthesized, characterized, and applied in the development of dye-sensitized solar cells (DSSCs). It was found that the nature of the *para*-substituent affects the behavior of these sensitizers. In particular, the introduction of a C11 linear fluorous alkoxy group led to an improvement in the power conversion efficiency with respect to the commonly employed nonfluorous alkoxy substituents.

.

Introduction

A great deal of research is currently being conducted in the field of dye-sensitized solar cells (DSSCs) based on the sensitization of a nanostructured metal oxide semiconductor interface by a photoexcited dye.[1,2] Many different issues are addressed, ranging from the comprehension and modeling of the underlying fundamental phenomena to the assessment of the life cycle and economic effectiveness of the final devices.[3-8] However, the development of new photosensitizers that could ensure optimal photovoltaic parameters and acceptable lifetime service to DSSCs remains a major goal in this field, despite the impressive number of light-absorbing compounds with different molecular structures already proposed and tested.[2,9-12] Encouraging results have been obtain in the case of structurally simple dipolar organic dyes comprising an electron-rich donor component (D) and an electron-withdrawing acceptor counterpart (A) bridged by a π-conjugated linkage. Such a flexible D-π-A modular blueprint allows for a great diversity of conceivable molecular structures. Organic sensitizers with tailored optical and energetic properties, high molar extinction coefficients and long term chemical stability have been thus synthesized through the judicious combination of the three basic D, π and A elements.[13] In practice,

triarylamine derivatives and cyanoacrylic acid, which also works as the anchoring group to the metal oxide electrode, have been the most commonly used D and A components, respectively, while the nature of the π-conjugated unit has been more systematically modified. This last parameter has a deep influence on the final performance of the dye, as it modulates the absorption of solar light and the ability to inject electrons to the metal oxide conduction band from photoinduced intramolecular charge transfer states produced upon irradiation of the dipolar molecule. Therefore, the inclusion of different π-conjugated cores such as simple C-C double or triple bonds, aryl or heteroaromatic rings, or combinations of all these elements has been widely investigated.[14] The adoption of this strategy proved to be instrumental in providing highly efficient organic dyes that contributed to fabricate DSSCs with photovoltaic performances close to those obtained using well-established Ru-based sensitizers.[15-17]

The basic D-π-A molecular design has some drawbacks, too. Besides the inherent aggregation tendency shown by many rod-like shaped D-π-A dyes,[13,14] the presence of a single accepting/anchoring A group results in a reduced interfacial electron transfer ability and higher propensity to detach from the semiconductor surface under operating conditions. The incorporation of the most successful dipolar structural motifs into multi-branched, multi-anchoring molecular architectures (Figure 1a) can help to relieve these problems, as early demonstrated by Abbotto *et al.* who first designed di-anchoring dyes of the form D-(π-A)₂, where two branches stem from the same D unit.[18] Following this line of reasoning, several research groups devised other D-(π-A)₂ dyes containing variously substituted arylamines, carbazoles, phenothiazines or phenoxazines as D units,[19,20] as well as more exotic X- and Y-shaped dyes, such as spiro-configured molecules where two identical D-π-A branches are interconnected by a common sp³-

[a.] Department of Chemical, Toxicological and Pharmacological Evaluation of Drugs, Faculty of Pharmacy, Catholic University Our Lady of Good Counsel, Rr. D. Hoxha, Tirana, Albania

[b.] Departamento de Química, Universidad Nacional de Río Cuarto. CONICET, Agencia Postal No 3, X5804BYA, Río Cuarto, Argentina. E-mail: ffungo@exa.unrc.edu.ar

[c.] Istituto di Scienze e Tecnologie Molecolari del Consiglio Nazionale delle Ricerche, ISTM-CNR, Via Golgi 19, 20133 Milano, Italy. E-mail: gianluca.pozzi@istm.cnr.it

carbon atom.[21-23] Nevertheless, the design of multi-branched, multi-anchoring dyes remains a relatively underdeveloped field and there is much room for further research on the optimization of the D, π and A components and their integration into new molecular architectures through the application of suitable synthetic schemes.

In preceding works, we demonstrated the use of fluorene as the π-conjugated central core of multi-branched spiro-configured (D-π-A)$_2$-sensitizers.[21,22] Here, it is shown that fluorene can play a similar role in D-(π-A)$_2$ molecules (Figure 1b), and that the photovoltaic performance of di-branched, di-anchoring sensitizers can be improved through the introduction of linear perfluorinated (fluorous) alkoxy substituents in the *para*-position of the central D unit.
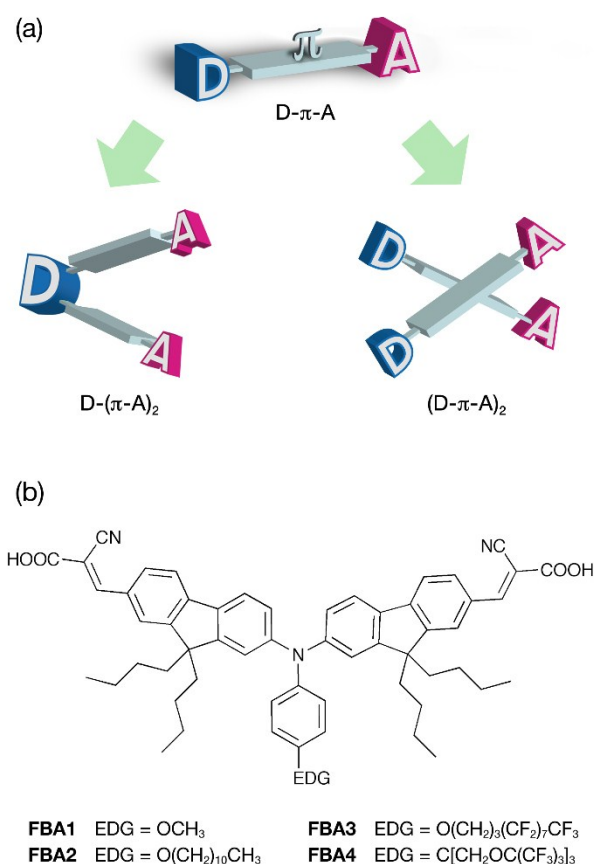

Figure 1. (a) General structure of D-(π-A)$_2$ and X-shaped, spiro-configured dyes for DSSCs; (b) D-(π-A)$_2$ fluorene-based dyes synthesized in this work.

Results and discussion

Synthesis of dyes

Arylamine donors and cyanoacrylic acid acceptors are the most widely used structural units in D-(π-A)$_2$ sensitizers,[19] similarly to conventional dipolar D-π-A dyes. This feature was maintained in the design of the fluorene-based **FBA1**-**FBA4** (Figure 1). On the other hand, fluorene is a useful building-block for the construction of dipolar sensitizers,[24-26] but its incorporation as π-conjugated unit in D-(π-A)$_2$ dyes for DSSCs has never been described. A convenient general approach based on the *N*-

functionalization of a versatile bis(fluorenyl)amine intermediate has been developed and applied to the synthesis of **FBA1**-**FBA4** (Scheme 1).

In brief, the Cu-catalyzed C-N coupling reaction between *tert*-butyl carbamate and a fourfold molar excess of the starting material **1**, readily obtained by alkylation of commercially available 2,7-dibromofluorene, afforded the Boc-protected secondary amine **2** in 56% yield, while the unreacted dibromo fluorene was recovered and reused. Bis-lithiation/electrophilic quench of **2** gave the bis-aldehyde **3** (82% yield) from which amine **4** was readily released by acid cleavage in 89% yield. Pd-catalyzed cross-coupling of this bis(fluorenyl)amine intermediate with suitable aryl halides, followed by Knoevenagel condensation with cyanoacetic acid, led to the desired D-(π-A)$_2$ dyes. This synthetic pathway enables the introduction of a great variety of substituents on their arylamine D unit and therefore the possible fine-tuning of their ultimate behaviour as sensitizers in DSSCs, as it appears from a thorough analysis of literature data.[19] In this regard, the presence of electron-donating *para*-alkoxy substituents is a common feature of many effective multi-branched, multi-anchoring dyes based on arylamines. We thus decided to investigate the effect of similar substituents on the behaviour of the D-(π-A)$_2$ dyes derived from **4**. Dyes **FBA1** and **FBA2** bearing standard short (*p*-OMe) and long (*p*-OC$_{11}$H$_{23}$) chain substituents, respectively, where obtained using known aryl halides. The unusual fluorous substituents present in dyes **FBA3** and **FBA4** were introduced thanks to the use of two purposely synthesized aryl halides (see ESI).

Photophysical and electrochemical characterization

The photophysical properties of the branched dyes were evaluated in solvent media with different polarity, namely toluene (TOL), 1,2-dichloroethane (DCE) and acetonitrile (MeCN). As shown in Figure 2 and summarized in Table 1, all dyes display three main absorption bands in DCE solution, two of which are in the near UV region (λ$_{max}$ at ≈320 and ≈350 nm) and may be attributed to π-π* transitions in the fluorene system. The third and more intense band, corresponding to an intramolecular charge transfer (ICT) transition, is observed at lower energy (λ$_{max}$ at ≈480-500 nm). The ICT character of this band was confirmed by the fluorescence solvatochromism observed when solvents with different polarity were investigated. The four dyes under study showed a marked batochromic displacement when the polarity of the solvent was increased (see Figure 2 and Table 1). For example, the maximum emission of **FBA3** was shifted 134 nm to lower energy when TOL was changed for MeCN. On the other hand, comparison of the absorption spectra of the four dyes in the same solvent (e.g. DCE, Table 1) revealed that the ICT light absorption band maximum for **FAB4** has higher energy values (blue shift ≈15 nm) with respect to the other dyes, which share most of the structural features with **FBA4**, except for the nature of the *para*-substituent of the central D unit (Figure 2).
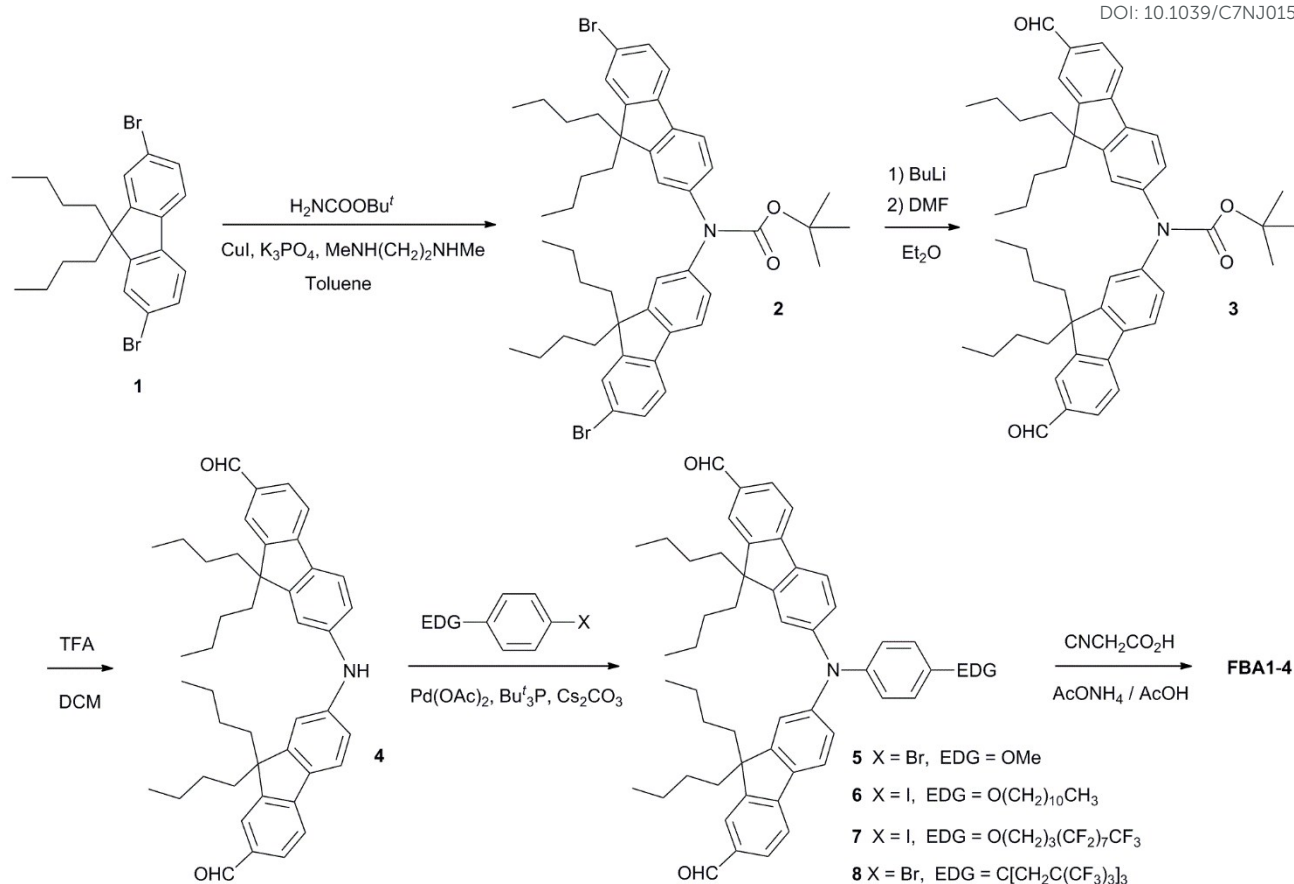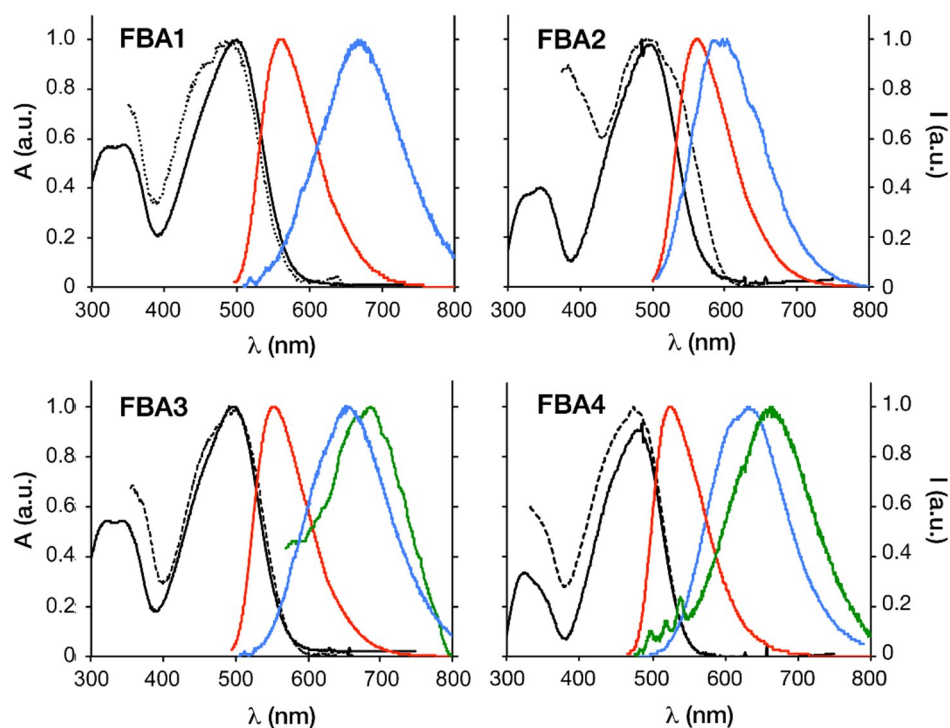
Scheme 1. Synthesis of fluorene-based D-(π-A)₂ dyes.

Figure 2. Normalized UV-Vis absorption spectra (black solid line) and excitation spectra (black dashed line) of the dyes in DCE solution. Normalized emission spectra of the dyes in DCE (light-blue solid line), TOL (red solid line) and MeCN (green solid line) solution. Emission spectra were measured by excitation at the maximum of the respective ICT bands.

The observed trend can be thus related to the presence of *para*-alkoxy substituents in **FAB1**, **FAB2** and **FAB3**, which increases the electron density on the amino group stabilizing the photogenerated positive charge. It can be also noted that the insertion of a propylene spacer between the oxygen atom and the linear perfluoroalkylated C8-chain offers an effective insulation against the electron-withdrawing effect of the latter. Indeed, the ICT band maxima of **FAB3** and **FBA2** are fully comparable.

Table 1. Optical and electrochemical characteristics of the studied dyes

	λ_{max} Absorption (nm)	λ_{max} Emission (nm)[a]			$E_{1/2}$ (V)[b]
	DCE	TOL	DCE	MeCN	
FBA1	320/349/500	559	669	-[c]	0.33
FBA2	322/348/494	561	596	-[c]	0.35
FBA3	318/345/495	552	655	686	0.34
FBA4	323/351/482	525	633	662	0.51

[a] Emission spectra were measured by excitation at the maximum of the respective ICT bands. [b] Potential values relative to Fc/Fc+ redox couple (0.40 V vs SCE). [c] Low solubility hampers light emission measurements.

The dyes excitation spectra in DCE solution are also shown as black dashed lines in Figure 2. The observed similarity between the excitation and absorption spectra indicates that all the excited states contribute to the formation the ICT processes.

Finally, the UV-Vis absorption spectra of the adsorbed sensitizers on TiO2 porous electrodes fit well with the corresponding spectra in solution (see ESI, Figure S1). As expected, the ICT band looks broader and shows a small maximum wavelength displacement with respect to the spectrum in solution due to the interaction of the dye molecules with the TiO2 surface and among themselves. All these optical characteristics are in agreement with related structures and highly desirable from the DSSC point of view.[21,26]

Cyclic voltammetric measurements were performed to study the electrochemical behaviour of the new sensitizers. All four compounds exhibit a typical quasi-reversible oxidation wave, which is related to the oxidation of the arylamine group (see ESI, Figure S2). The calculated oxidation half wave potentials ($E_{1/2}$) are summarized in Table 1. As in the case of optical properties, the observed differences in oxidation potentials are directly related to the molecular structures of the compounds under study and can be similarly analyzed. **FBA4** shows the highest $E_{1/2}$ value (0.51 V), while **FBA1**, **FBA2** and **FBA3** are ≈0.15 V easier to oxidize, with similar $E_{1/2}$ values among them, because of the presence of p*ara*-alkoxy substituents that are able to stabilize the generated positive charge.[26] The electron-withdrawing fluorous chain attached to **FBA3** do not affect the oxidation process thanks to the efficient electronic shielding provided by the propylene spacer.

Starting from the experimental optical and electrochemical parameters discussed above, the energy level diagram shown in Figure 3 was built, from which the energetic feasibility of the DSSC process could be evaluated. The comparison of the energy levels of the ground and excited states of the dyes with the redox potential of the iodine couple and the lower edge of the

conduction band of TiO2 revealed that in all cases the expected electron flow (injection into TiO2 from dye excited state and dye regeneration by the I−/I3− couple) is exothermic, thus making DSSC operation viable.
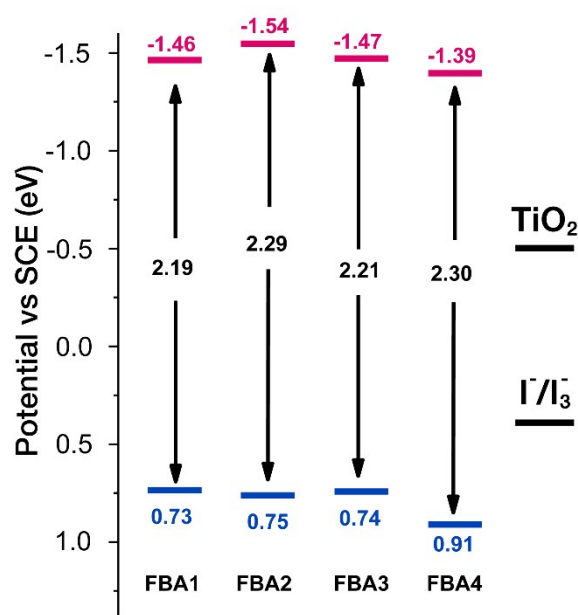

Figure 3. Energy level diagram of the studied dyes. Oxidation potentials in the ground and excited states are reported. The redox potential of the iodide/triiodide couple and the lower edge of the conduction band of TiO2 are introduced for comparison.

Computational analysis

The optimized spatial configuration of the di-branched **FBA** dyes and the frontier molecular orbitals were determined by semiempirical AM1 calculations (HyperChem package). Representative results relative to the fluorous dyes **FBA3** and **FBA4** are shown in Figures 4a-f. In both cases the two fluorene branches connected to the central aryl amino group are extended apart from each other due to sp3 hybridization of the nitrogen atom (Figures 4a-b). Accordingly, both branches are capable of interaction with the TiO2 surface through the cyanoacrylic end groups. This conclusion was further corroborated by comparison of FT-IR spectroscopy data obtained from **FBA3** dispersed in KBr pellets or adsorbed on TiO2. In this last case the spectra revealed that the characteristic band at 1691 cm-1 assigned to the free carboxylic acid groups of the KBr dispersed dye entirely vanishes, thus providing clear indication of the double-anchoring behaviour (see ESI, Figure S3).[21,22,27]

Figures 4c-d show that the HOMOs of **FBA3** and **FBA4** are localized mostly around the central aryl amino groups, whereas the LUMOs (Figures 4e-f) are localized on the cyanoacrylic residues, regardless of the kind of fluorous substituent. Therefore, it is expected that upon photoexcitation the electron distributions are moved from the donor units (ground state) to the acceptor units, close to the anchoring groups, which favour the electron injection from the dye molecules to the TiO2 conduction band edge.
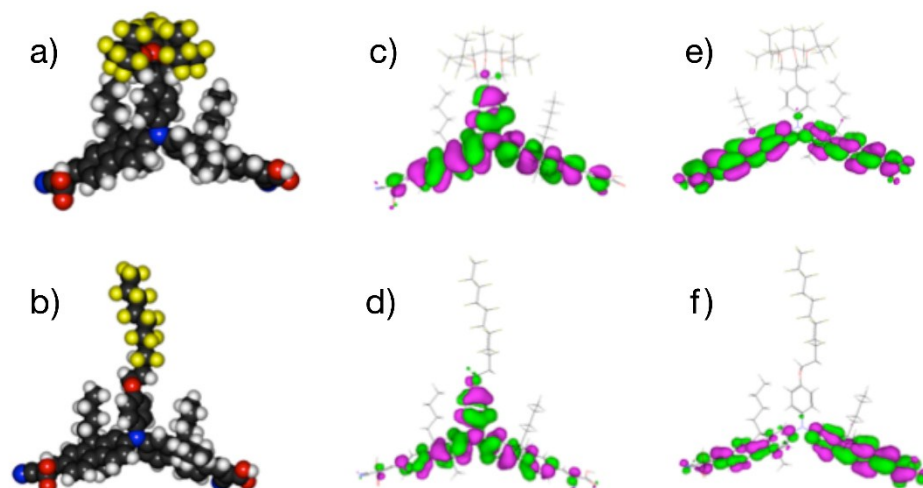
Figure 4. Geometric optimization (AM1 semiempirical calculations at HyperChem software) of the dyes **FBA4** (upper panels) and **FBA3** (lower panels): a-b spatial configuration, c-d HOMO and e-f LUMO molecular orbitals.

It must be also noted that the bulky fluorous domain (nine CF_3 groups) present in **FBA4** forms a sort of hydrophobic/lipophobic umbrella over the donor group, which is oxidized upon the photoinduced charge transfer process (Figure 4a). This feature is not present in the other members of the dye series and can possibly hamper the regeneration of the reduced form of the dye during DSSC operation (see later).

Photovoltaic properties of DSSC devices

DSSC devices based on the donor-acceptor di-branched di-anchoring sensitizers were constructed in order to evaluate the photovoltaic performance of the **FBA** dyes. A common fabrication methodology, described in the experimental section, was employed, in order to fairly compare the fluorous and non-fluorous sensitizers. Additionally, all the fabricated cells exhibited similar light absorption in the visible range (electrode absorbance ~2 at λ = 470 nm), suggesting similar dye loading over TiO_2 surface. Fifteen batches of four cells were tested for each dye.
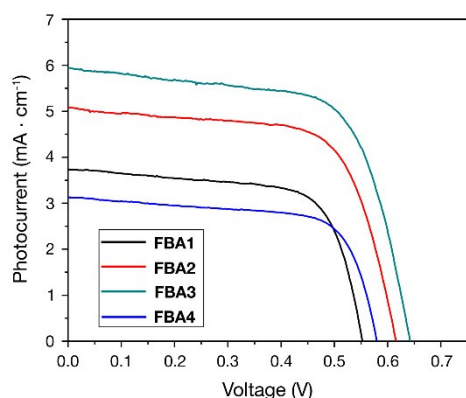

Figure 5. Photocurrent-voltage curves for di-anchoring D-(π-A)$_2$ photosensitizers.

Typical photocurrent–voltage (J/V) curves J curves are shown in Figure 5 while averaged values of the key photovoltaic parameters calculated from all devices are collected in Table 2. The measurement procedure of the J-V curves can affect the obtained DSSC parameters (short circuit photocurrent density, J_{SC}; open circuit photovoltage, V_{OC}; fill factor, FF; energy conversion efficiency, η), as discussed in recent literature examples.[28,29] Thus, in order to carry out a comparative analysis of the performance of the **FAB#** dyes series used in DSSC construction, and for avoid measurements procedure effects, we applied a voltage sweep from J_{SC} to V_{OC} at 5 mV/s scan rate, to ensure a steady state cell operation regime. This procedure minimize any hysteresis effect originated from chemical capacitance and series resistances in the DSSC.[28,29]

Both J_{sc} and V_{oc} values of DSSCs based on **FBA2** and **FBA3** dyes bearing long linear *para*-alkoxy substituents are clearly higher than those of DSSCs built with the *para*-alkoxy free **FBA4** dye, but also than those obtained in the case of **FBA1** that contains a simple –OMe substituent. Moreover, in all the analyzed batches of samples the cells constructed with the fluorous compound **FBA3** exhibited a short circuit photocurrent about 35% higher than those fabricated with the otherwise identical **FBA2** dye holding a linear hydrocarbon chain.

Table 2. DSSC performance data of di-anchoring D-(π-A)$_2$ photosensitizers.

	J_{sc} (mA/cm²)	V_{OC} (V)	FF	η (%)
FBA1	3.76	0.55	0.68	1.4
FBA2	5.05	0.61	0.68	2.1
FBA3	5.95	0.64	0.66	2.5
FBA4	3.07	0.58	0.70	1.2

We already reported that the presence of perfluoroalkyl substituents in fluorene centered D-π-A photosensitizers has a strong influence in the generation of photoelectric effects.[26] In particular, the introduction of branched fluorous groups in the tail D end of the molecular structure allowed to obtain higher

energy conversion efficiencies, due to the generation of larger photocurrent densities. This fact was ascribed to the anti-aggregation behaviour offered by the fluorous substituents, and to their efficient shielding effect on the TiO$_2$ surface that avoids deleterious back electron transfer to the iodine electrolyte. The present results confirm the beneficial effect of the presence of fluorous substituents on the donor moiety of D-(π-A)$_2$ sensitizers. However, a correct choice of the fluorous substituents is extremely important. Indeed, the fluorous dye **FBA4** was found to generate the lowest photocurrent and energy conversion efficiency values among the investigated dyes. Two major factors contribute to this behaviour, namely the absence of a direct ether bond between the aryl amino D unit and the fluorinated fragment, and the above mentioned stereochemical constraints. As can be seen in Figure 4a the phenyl amine donor group in **FBA4** is roofed over by the umbrella-like fluorous substituent. To ensure efficient DSSC operation, the donor group photo-oxidized upon light absorption and electron injection must be quickly reduced by the triiodide present in the electrolyte solution. The steric hindrance and the solvophobic environment produced by nine CF$_3$ groups can hamper the efficient redox reaction, with a consequent negative effect on the photocurrent generation, which is about one half of that obtained with the other fluorous dye **FBA3**.
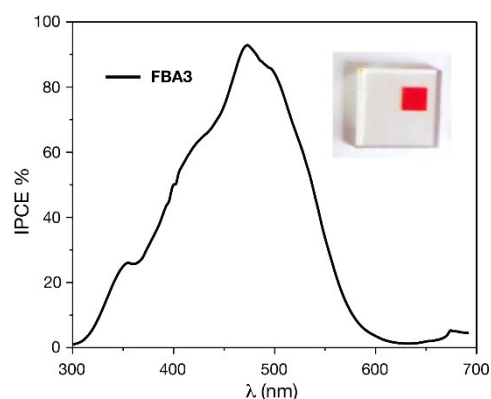

Figure 6. IPCE spectrum of the DSSC fabricated with the fluorous dye **FBA 3**.

The use of organic D-(π-A)$_2$ dyes based on fluorene subunits in DSSCs afforded photovoltaic performance inferior to those obtained with one of the most efficient and widely used photosensitizers, namely the Ru-based N719 dye.[30] For cells fabricated under the same experimental conditions, the latter ensured 5.2% energy conversion efficiency against the highest 2.5% value obtained using **FBA3**. Indeed, contrary to the black-coloured N719, the present D-(π-A)$_2$ photosensitizers are not panchromatic and absorb only a part of the solar, as exemplified in Figure 6 where a picture of the red photoelectrode containing **FBA3** and the corresponding incident photon to current efficiency (IPCE) spectrum are reported. The complete set of IPCE spectra for dyes **FAB1-4** is reported in Figure S4, ESI. In all cases the IPCE curves closely follow the absorption spectra of the corresponding dyes. Also, the IPCE maxima and device performance trends are in good agreement. The selective light harvesting behaviour of these dyes is likely resultant from the

reduced ability of the fluorene π-bridges to ensure electron delocalization between the donor and acceptor units.[31] This has a negative effect on the overall energy conversion efficiencies, but it is crucial for the fabrication of semitransparent, coloured solar cells of high interest from an architectural point of view and for the design and construction of smart windows in energy efficient modern buildings.[32,33]

Conclusions

A set of di-branched, di-anchoring organic photosensitizers D-(π-A)$_2$ comprising of two identical fluorene subunits attached to a pivotal aryl amino donor group has been synthesized. The photovoltaic performances of these new Y-shaped compounds in DSSCs are deeply influenced by the nature of the substituents present on the donor unit. In particular the introduction of the linear fluorous alkoxy substituent −O(CH$_2$)$_3$C$_8$F$_{17}$ ensures improved power conversion efficiency with respect to standard short- and long-chain electron-donating *para*-alkoxy substituents previously used in many effective multi-branched, multi-anchoring dyes based on arylamines.[19] The beneficial influence of fluorous groups was already observed in fluorene-based D-π-A photosensitizers and it was ascribed to a combination of reduced aggregation of the dye and efficient shielding of the titania surface, that avoids deleterious back electron transfer to the iodine electrolyte.[26] The same effects are likely to play a major role in the present case, since photophysical and electrochemical studies and frontier molecular orbitals calculations evidence the inherently similar electronic properties of the fluorous and non-fluorous *para*-alkoxy-substituted dyes. This is a useful clue for future improvements in dye molecular design. At the same time, the introduction of a spherical-shaped, bulky fluorous substituent connected to the donor unit through a C-C bond has detrimental consequences that are possibly related to both electronic factors and to an excessive steric hindrance. Such a behaviour was not observed in the case of linear D-π-A photosensitizer based on fluorene and should be also taken into account in the future development of multi-branched, multi-anchoring molecular architectures containing fluorous components.

Experimental

Materials and methods

Chemicals. All commercially available products were used as received without further purification. 2,7-Dibromo-9,9-dibutyl-9*H*-fluorene **1** was prepared as described in the literature.[34] Synthesis details for 1-Iodo-4-(undecyloxy)benzene, 1-iodo-4-(4,4,5,5,6,6,7,7,8,8,9,9,10,10,11,11,11-heptadecafluoroundecyloxy)benzene and 1-(1,3-bis(1,1,1,3,3,3-hexafluoro-2-(trifluoromethyl)propan-2-yloxy)-2-((1,1,1,3,3,3-hexafluoro-2-(trifluoromethyl)propan-2-yloxy)methyl)propan-2-yl)-4-bromobenzene are provided in the Electronic Supporting Information. Solvents were purified by standard methods and dried if necessary. Reactions were

monitored by thin layer chromatography (TLC) that was conducted on plates precoated with silica gel Si 60-F254 (Merck, Germany). Column chromatography was carried out on silica gel SI 60 (Merck, Germany), mesh size 0.063 – 0.200 mm (normal) or 0.040 – 0.063 mm (flash). ^{1}H NMR and ^{13}C NMR were recorded on a Bruker Avance 400 spectrometer (400 and 100.6 MHz, respectively); ^{19}F NMR spectra were recorded on a Bruker AC 300 spectrometer (282 MHz). ESI mass spectra were obtained with an ICR-FTMS APEX II (Bruker Daltonics) mass spectrometer. Elemental analyses were carried out by the Departmental Service of Microanalysis (University of Milano).

Photophysical and electrochemical characterization of dyes. Absorption and fluorescence spectra were recorded on a Shimadzu UV-2401PC spectrometer and on a Spex FluoroMax fluorometer, respectively Spectra were acquired using quartz cells (path length: 1 cm) at room temperature in 1,2-dichloroethane (DCE), acetonitrile (MeCN) and toluene (TOL) solutions. To obtain the absorption spectra of the dyes adsorbed on titanium oxide, a diffuse reflectance cell (integrating sphere) was added to the Shimadzu UV-2401PC spectrometer. Electrochemical properties of the dyes were determined using an Autolab Electrochemical Workstation PGSTAT 30 provided with a conventional three electrodes cell with a Pt disk, silver wire and Pt coil as working reference and counter electrodes, respectively. A deoxygenated 0.10 M solution of tetra-n-butylammonium hexafluorophosphate (TBAPF$_6$) in DCE containing 1 mmol of salt was used as the supporting electrolyte for all dyes. The Pt working electrode was polished between experiments with 0.3 mL of alumina paste and sequentially sonicated in water and absolute ethanol. Ferrocene was used as an internal standard. Therefore, all the potential values are reported relative to Fc/Fc$^+$ redox couple (0.40 V vs SCE).[35]

DSSC preparation and characterization. The assembly of the dye-sensitized solar cells was performed using a commercial Solaronix test cell kit, with the purpose of standardizing the operations and performing comparative studies based on multiple samples. The kit was composed by a fluorine-doped tin oxide (FTO) glass covered by screen printing with Solaronix Titanium Oxide pastes (active layer of Ti-Nanoxide T/SP covered by a reflective layer of Ti-Nanoxide R/SP, active area: 6 x 6 mm), platinized electrodes (FTO glass with a homogeneous surface of the precursor Platisol T/SP), a sealing film made of Meltonix 1170-60, a slim glass and Iodolyte Z-50 Solaronix as redox electrolyte. Dye-coating of the TiO$_2$ films was carried out by soaking the films in 10^{-3} M solution of dye in absolute ethanol, after heating the electrode to 60 ^{0}C. The two electrodes were laminated together using Meltonix 1170-60 and the solar cell was filled with Iodolyte Z-50 through a hole in the cathode. The filling hole was then sealed with Meltonix 1170-60 and a thin circle glass of 6 mm diameter.

Photocurrent spectra were obtained by illumination of the solar cell with monochromatic light obtained from a 75-W high-pressure Xe lamp (Photon Technology Instrument, PTI) and a monochromator equipped with a stepper motor controlled by a personal computer. The incident light intensities at different wavelengths were measured with a Coherent Laser-Mate Q

radiometer. The photocurrent and voltage were measured using a solar simulator (Sciencetech 150) equipped with an AM 1.5 G filter. The reported data are average values of a series of at least fifteen cells for each dye.

Synthetic procedures

Synthesis of *tert*-butyl bis(7-bromo-9,9-dibutyl-9*H*-fluoren-2-yl)carbamate (2). A flame-dried Schlenk tube was charged with 2,7-dibromo-9,9-dibutyl-9*H*-fluorene **1** (1.74 g, 4.0 mmol), CuI (38 mg, 0.2 mmol), *tert*-butyl carbamate (117 mg, 1.0 mmol) and K$_3$PO$_4$ (0.85 g, 4.0 mmol), evacuated, and backfilled with nitrogen. *N,N*-Dimethylethylenediamine (90 µL, 0.8 mmol) and dry toluene (8 mL) were added under nitrogen. The Schlenk tube was sealed and the reaction mixture was stirred at 110 °C for 24 h. The resulting suspension was allowed to reach room temperature and filtered through a short pad of Celite. The filtrate was evaporated under reduced pressure and the residue was purified by flash column chromatography (silica gel, hexane/AcOEt 95/5) affording compound **2** as a white solid. Yield: 466 mg (56%). Mp = 212 °C. ^{1}H NMR (400 MHz, CDCl$_3$): δ [ppm] = 7.55 (d, J = 8.1 Hz, 2H), 7.52 – 7.47 (m, 2H), 7.46 – 7.41 (m, 4H), 7.20 – 7.12 (m, 4H), 1.88 (m, 8H), 1.47 (s, 4H), 1.13 – 0.99 (m, 4H), 0.66 (t, J = 7.3 Hz, 6H), 0.59 (m, 4H). ^{13}C NMR (100.6 MHz, CDCl$_3$): δ [ppm] = 153.8, 153.2, 151.0, 143.0, 139.7, 137.5, 130.2, 126.2, 125.6, 121.9, 121.1, 121.0, 120.0, 81.2, 55.4, 40.1, 28.5, 26.0, 23.1, 14.0. Anal. Calcd. for C$_{47}$H$_{57}$Br$_2$NO$_2$: C 68.20, H 6.94, N 1.69. Found: C 68.18, H 6.97, N 1.65.

Synthesis of *tert*-butyl bis(9,9-dibutyl-7-formyl-9*H*-fluoren-2-yl)carbamate (3). A solution of *n*-butyl lithium in hexane (1.6 M, 2.0 mL, 3.2 mmol) was added dropwise over 10 min to a stirred solution of compound **2** (0.83 g, 1.0 mmol) in dry THF (9 mL) at -78 °C under nitrogen. The resulting mixture was stirred for an additional hour at this temperature, then dry DMF (0.24 mL, 3.0 mmol) was added dropwise. The final reaction mixture was allowed to attain room temperature and stirred 2 h, followed by quenching with 5% aq. HCl (3 mL) and extraction of the aqueous phase with Et$_2$O (3 × 10 mL). The combined organic layers were washed with H$_2$O, brine and dried over MgSO$_4$. The solvent was evaporated under reduced pressure and the residue was purified by flash column chromatography (silica gel, hexane/AcOEt 85/15) affording compound **3** as a pale yellow solid. Yield: 595 mg (82%). Mp = 205 °C. ^{1}H NMR (400 MHz, CDCl$_3$): δ [ppm] = 10.05 (s, 2H), 7.86 – 7.84 (m, 4H), 7.78 (d, J = 8.2 Hz, 2H), 7.69 (d, J = 8.2 Hz, 2H), 7.26 (d, J = 2.7 Hz, 2H), 7.21 (dd, J = 8.2, 1.9 Hz, 2H), 2.09 – 1.87 (m, 8H), 1.48 (s, 9H), 1.12 – 0.99 (m, 8H), 0.65 (t, J = 7.3 Hz, 12H), 0.62 – 0.47 (m, 8H). ^{13}C NMR (100.6 MHz, CDCl$_3$): δ [ppm] = 192. 5, 153.6, 152.9, 151.8, 147.0, 144.0, 137.1, 135.3, 130.9, 125.8, 123.1, 122.0, 121.3, 120.0, 81.6, 55.4, 40.0, 28.4, 26.1, 23.1, 14.0. Anal. Calcd. for C$_{49}$H$_{59}$NO$_4$: C 81.06, H 8.19, N 1.93. Found: C 81.00, H 8.25, N 1.91.

Synthesis of bis(9,9-dibutyl-7-formyl-9*H*-fluoren-2-yl)amine (4). To a stirred solution of carbamate **3** (0.73 g, 1.0 mmol) in dry DCM (6 mL) cooled to 10 °C trifluoroacetic acid (6 mL) was added dropwise under nitrogen. The solution was stirred 3 h at room

temperature after which the volatiles were eliminated under reduced pressure. The residue was dissolved in DCM and the solution was washed with H_2O, 5% aq. NaOH, H_2O, brine and dried over $MgSO_4$. The solvent was evaporated under reduced pressure and the residue was purified by flash column chromatography (silica gel, petroleum ether/AcOEt 4/1) affording compound **4** as a yellow solid. Yield: 557 mg (89%). Mp = 163 °C (dec.). ^{1}H NMR (400 MHz, CD_2Cl_2): δ [ppm] = 10.03 (s, 2H), 7.86 – 7.84 (m, 4H), 7.77 (d, J = 8.2 Hz, 2H), 7.74 (d, J = 8.2 Hz, 2H), 7.26 (d, J = 1.9 Hz, 2H), 7.12 (dd, J = 8.2, 2.0 Hz, 2H), 6.35 (s, 1H), 2.11 – 1.92 (m, 8H), 1.17 – 1.08 (m, 8H), 0.71 (t, J = 7.5 Hz, 12H), 0.70 – 0.58 (m, 8H). ^{13}C NMR (100.6 MHz, CD_2Cl_2): δ [ppm] = 192.5, 154.7, 151.4, 148.2, 144.2, 135.1, 133.6, 131.1, 123.5, 122.7, 119.4, 117.7, 112.2, 55.7, 40.77, 26.6, 23.6, 14.2. Anal. Calcd. for $C_{44}H_{51}NO_2$: C 84.44, H 8.21, N 2.24. Found: C 84.41, H 8.22, N 2.15.

Synthesis of N,N-bis(9,9-dibutyl-7-formyl-9H-fluoren-2-yl)-N-(4-methoxyphenyl)amine (5). A flame-dried Schlenk tube was charged with compound **4** (188 mg, 0.3 mmol), 4-bromoanisole (22 μL, 0.5 mmol), Cs_2CO_3 (652 mg, 2.0 mmol) and $Pd(OAc)_2$ (12 mg, 0.05 mmol), evacuated, and backfilled with nitrogen. Dry, degassed toluene (7 mL) and P[t]Bu₃ (1 M in toluene, 100 μL, 0.1 mmol) were subsequently added under nitrogen. The Schlenk tube was sealed and the reaction mixture was stirred at 110 °C for 24 h. After cooling to room temperature the reaction mixture was diluted with DCM and filtered through a short pad of Celite. The filtrate was evaporated under reduced pressure and the residue was purified by flash column chromatography (silica gel, petroleum ether/DCM 1/1) affording compound **5** as a yellow foam. Yield: 158 mg (72%). ^{1}H NMR (400 MHz, $CDCl_3$): δ [ppm] = 10.03 (s, 2H), 7.84 – 7.82 (m, 4H), 7.73 (d, J = 8.2 Hz, 2H), 7.61 (d, J = 8.3 Hz, 2H), 7.17 – 7.12 (m, 4H), 7.06 (dd, J = 8.3, 2.0 Hz, 2H), 6.88 (d, J = 9.0 Hz, 2H), 3.84 (s, 3H), 2.06 – 1.80 (m, 8H), 1.15 – 1.04 (m, 8H), 0.71 (t, J = 7.3 Hz, 12H), 0.68 – 0.54 (m, 8H). ^{13}C NMR (100.6 MHz, $CDCl_3$): δ [ppm] = 192.4, 156.8, 153.9, 151.3, 148.8, 147.6, 140.6, 134.7, 134.0, 131.0, 127.5, 123.0, 122.1, 121.8, 119.2, 117.3, 115.0, 55.7, 55.3, 40.0, 26.2, 23.1, 14.1. Anal. Calcd. for $C_{51}H_{57}NO_3$: C 83.68, H 7.85, N 1.91. Found: C 83.70, H 7.89, N 1.89.

Synthesis of N,N-bis(9,9-dibutyl-7-formyl-9H-fluoren-2-yl)-N-(4-undecyloxyphenyl)amine (6). A flame-dried Schlenk tube was charged with compound **4** (94 mg, 0.15 mmol), 1-iodo-4-(undecyloxy)benzene (93 mg, 0.25 mmol), Cs_2CO_3 (407 mg, 1.25 mmol) and $Pd(OAc)_2$ (5.6 mg, 0.025 mmol), evacuated, and backfilled with nitrogen. Dry, degassed toluene (4 mL) and P[t]Bu₃ (1 M in toluene, 50 μL, 0.05 mmol) were subsequently added under nitrogen. The Schlenk tube was sealed and the reaction mixture was stirred at 110 °C for 20 h. After cooling to room temperature the reaction mixture was diluted with DCM and filtered through a short pad of Celite. The filtrate was evaporated under reduced pressure and the residue was purified by flash column chromatography (silica gel, hexane/Et₂O 4/1) affording compound **6** as a yellow foam. Yield: 115 mg (89%). ^{1}H NMR (400 MHz, $CDCl_3$): δ [ppm] = 10.03 (s, 2H),

7.84 – 7.80 (m, 4H) 7.72 (d, J = 8.2 Hz, 2H), 7.60 (d, J = 8.3 Hz, 2H), 7.14 – 7.10 (m, 4H), 7.06 (dd, J = 8.3, 2.0 Hz, 2H), 6.87 (d, J = 8.5 Hz, 2H), 3.97 (t, J = 6.5 Hz, 2H), 2.01 – 1.94 (m, 4H), 1.89 – 1.77 (m, 6H), 1.52 – 1.42 (m, 2H), 1.39 – 1.28 (m, 14H), 1.17 – 1.02 (m, 8H), 0.88 (t, J = 6.8 Hz, 3H), 0.71 (t, J = 7.3 Hz, 12H), 0.69 – 0.53 (m, 8H). ^{13}C NMR (100.6 MHz, $CDCl_3$): δ [ppm] = 192.3, 156.3, 153.7, 151.1, 148.7, 147.5, 140.2, 134.5, 133.8, 130.9, 127.4, 122.8, 122.0, 121.6, 119.1, 117.1, 115.4, 68.3, 55.1, 39.9, 31.9, 29.6, 29.5, 29.4, 26.1, 23.0, 22.7, 14.1, 13.9. Anal. Calcd. for $C_{61}H_{77}NO_3$: C 83.99, H 8.90, N 1.61. Found: C 83.80, H 8.96, N 1.57.

Synthesis of N,N-bis(9,9-dibutyl-7-formyl-9H-fluoren-2-yl)-N-(4,4,5,5,6,6,7,7,8,8,9,9,10,10,11,11,11-heptadecafluoroundecyloxy)amine (7). A flame-dried Schlenk tube was charged with compound **4** (94 mg, 0.15 mmol), 1-iodo-4-(4,4,5,5,6,6,7,7,8,8,9,9,10,10,11,11,11-heptadecafluoroundecyloxy)benzene (170 mg, 0.25 mmol), Cs_2CO_3 (407 mg, 1.25 mmol) and $Pd(OAc)_2$ (5.6 mg, 0.025 mmol), evacuated, and backfilled with nitrogen. Dry, degassed toluene (4 mL) and P[t]Bu₃ (1 M in toluene, 50 μL, 0.05 mmol) were subsequently added under nitrogen. The Schlenk tube was sealed and the reaction mixture was stirred at 110 °C for 8 h. After cooling to room temperature the reaction mixture was diluted with DCM and filtered through a short pad of Celite. The filtrate was evaporated under reduced pressure and the residue was purified by column chromatography (silica gel, DCM) affording compound **7** as a yellow foam. Yield: 117 mg (66%). ^{1}H NMR (400 MHz, $CDCl_3$): δ [ppm] = 10.03 (s, 2H), 7.84-7.82 (m, 4H), 7.73 (d, J = 8.3 Hz, 2H), 7.61 (d, J = 8.3 Hz, 2H), 7.16 – 7.11 (m, 4H), 7.05 (dd, J = 8.3, 2.0 Hz, 2H), 6.87 (d, J = 8.9 Hz, 2H), 4.06 (t, J = 5.8 Hz, 2H), 2.46 – 2.26 (m, 2H), 2.19 – 2.08 (m, 2H), 2.05 – 1.92 (m, 4H), 1.91 – 1.79 (m, 4H), 1.17 – 1.01 (m, 8H), 0.70 (t, J = 7.3 Hz, 12H), 0.62 (m, 8H). ^{13}C NMR (100.6 MHz, $CDCl_3$): δ [ppm] = 192.3, 155.5, 153.7, 151.1, 148.6, 147.5, 140.8, 134.5, 133.9, 130.9, 127.3, 122.8, 122.1, 121.7, 119.1, 117.2, 115.4, 66.6, 55.1, 39.9, 28.0 (t, J_{CF} = 22 Hz), 26.1, 23.0, 20.6, 13.9. ^{19}F NMR (282 MHz, $CDCl_3$): δ [ppm] = -81.2 (t, J = 9.6 Hz, 3F), -114.7 (br s, 2F), -122.0 – -122.3 (m, 6F), -123.1 (br s, 2F), -123.8 (br s, 2F), -126.5 (br s, 2F). Anal. Calcd. for $C_{61}H_{60}F_{17}NO_3$: C 62.19, H 5.13, N 1.19. Found: C 62.31, H 5.27, N 1.12.

Synthesis of N,N-bis(9,9-dibutyl-7-formyl-9H-fluoren-2-yl)-N-(4-(1,3-bis(1,1,1,3,3,3-hexafluoro-2-(trifluoromethyl)propan-2-yloxy)-2-((1,1,1,3,3,3-hexafluoro-2-(trifluoromethyl)propan-2-yloxy)methyl)propan-2-yl)phenyl)amine (8). A flame-dried Schlenk tube was charged with compound **4** (94 mg, 0.15 mmol), 1-(1,3-bis(1,1,1,3,3,3-hexafluoro-2-(trifluoromethyl)propan-2-yloxy)-2-((1,1,1,3,3,3-hexafluoro-2-(trifluoromethyl)propan-2-yloxy)methyl)propan-2-yl)-4-bromobenzene (229 mg, 0.25 mmol), Cs_2CO_3 (407 mg, 1.25 mmol) and $Pd(OAc)_2$ (5.6 mg, 0.025 mmol), evacuated, and backfilled with nitrogen. Dry, degassed toluene (4 mL) and P[t]Bu₃ (1 M in toluene, 50 μL, 0.05 mmol) were subsequently added under nitrogen. The Schlenk tube was sealed and the reaction mixture was stirred at 110 °C for 24 h. After cooling to room temperature the reaction mixture was diluted with Et₂O and filtered through a short pad of Celite. The filtrate was

evaporated under reduced pressure and the residue was purified by flash column chromatography (silica gel, hexane/Et$_2$O 4/1) affording compound **8** as a yellow foam. Yield: 140 mg (64%).^{1}H NMR (400 MHz, CDCl$_3$): δ [ppm] = 10.04 (s, 2H), 7.87 – 7.83 (m, 4H), 7.75 (d, J = 8.4 Hz, 2H), 7.65 (d, J = 8.3 Hz, 2H), 7.21 – 7.12 (m, 6H), 7.07 (dd, J = 8.2, 2.0 Hz, 2H), 4.40 (s, 6H), 2.05 – 1.93 (m, 4H), 1.91 – 1.76 (m, 4H), 1.15 – 1.00 (m, 8H), 0.70 (t, J = 7.3 Hz, 12H), 0.67 – 0.55 (m, 8H). ^{13}C NMR (100.6 MHz, CDCl$_3$): δ [ppm] = δ 192.3, 153.8, 151.2, 148.0, 147.2, 147.1, 134.9, 134.8, 130.8, 130.6, 126.9, 124.2, 123.2, 122.9, 121.8, 120.1 (q, J_{CF} = 293 Hz), 119.3, 118.4, 79.4 (m), 68.1, 55.2, 48.0, 39.7, 26.1, 22.9, 13.8. ^{19}F NMR (282 MHz, CDCl$_3$): δ [ppm] = -68.7 (s). Anal. Calcd. for C$_{66}$H$_{60}$F$_{27}$NO$_3$: C 54.29, H 4.14, N 0.96. Found: C 54.12, H 4.30, N 0.95.

Synthesis of FBA1. A solution of dialdehyde **5** (146 mg, 0.2 mmol), cyanoacetic acid (85 mg, 1 mmol), and ammonium acetate (15 mg, 0.2 mmol) in AcOH (10 mL) was stirred under reflux for 6 h. The solvent was evaporated under reduced pressure, and the residue was taken up in DCM, washed extensively with H$_2$O, and dried over MgSO$_4$. After removal of the solvent at reduced pressure, the crude product was further purified by column chromatography (silica gel, DCM, and then DCM/AcOH 100/3) affording the title compound as a dark-red foam. Yield: 158 mg (91%). ^{1}H NMR (400 MHz, CDCl$_3$): δ [ppm] = 8.37 (s, 2H), 8.07 – 7.99 (m, 4H), 7.72 (d, J = 8.5 Hz, 2H), 7.62 (d, J = 8.3 Hz, 2H), 7.19 – 7.12 (m, 4H), 7.07 (dd, J = 8.4, 1.6 Hz, 2H), 6.90 (d, J = 9.0 Hz, 2H), 3.85 (s, 3H), 2.06 – 1.94 (m, 4H), 1.94 – 1.79 (m, 4H), 1.11 (m, 8H), 0.73 (t, J = 7.3 Hz, 12H), 0.69 – 0.57 (m, 8H). ^{13}C NMR (100.6 MHz, CDCl$_3$): δ [ppm] = 167.7, 157.0, 151.4, 147.4, 131.9, 129.1, 127.6, 125.9, 125.5, 121.8, 121.7, 119.6, 115.9, 116.6, 114.8, 99.0, 55.5, 55.3, 39.8, 26.1, 23.0, 13.9. λ$_{max}$(DCE)/nm 320 (ε/dm^3 mol^{-1} cm^{-1} 30817), 349 (27471) and 500 (50472). Anal. Calcd. for C$_{57}$H$_{59}$N$_3$O$_5$: C 79.05, H 6.87, N 4.85. Found: C 79.00, H 6.90, N 4.87. MS (ESI$^-$): m/z calcd. for C$_{57}$H$_{59}$N$_3$O$_5$: 865.4. Found 864.4 [M–H]$^-$..

Synthesis of FBA2. A solution of dialdehyde **6** (174 mg, 0.2 mmol), cyanoacetic acid (85 mg, 1 mmol), and ammonium acetate (15 mg, 0.2 mmol) in AcOH (10 mL) was stirred under reflux for 5 h. The solvent was evaporated under reduced pressure, and the residue was taken up in DCM, washed extensively with H$_2$O, and dried over MgSO$_4$. After removal of the solvent at reduced pressure, the crude product was further purified by column chromatography (silica gel, DCM, and then DCM/AcOH 95/1). The dark paste thus obtained was washed with cold petroleum ether affording the title compound as a dark-red foam. Yield: 177 mg (88%). ^{1}H NMR (400 MHz, CDCl$_3$): δ [ppm] = 8.37 (s, 2H), 8.09 – 7.95 (m, 4H), 7.72 (d, J = 8.4 Hz, 2H), 7.62 (d, J = 8.3 Hz, 2H), 7.22 – 7.00 (m, 6H), 6.89 (d, J = 8.9 Hz, 2H), 3.98 (t, J = 6.2 Hz, 2H), 2.07 – 1.77 (m, 10H), 1.58 – 1.45 (m, 2H), 1.41 – 1.25 (m, 14H), 1.19 – 1.03 (m, 8H), 0.89 (t, J = 6.7 Hz, 3H), 0.73 (t, J = 7.3 Hz, 12H), 0.70 – 0.54 (m, 8H). ^{13}C NMR (100.6 MHz, CDCl$_3$): δ [ppm] = 167.6, 157.1, 156.6, 154.0, 151.4, 148.9, 147.5, 139.9, 133.7, 132.1, 129.0, 127.7, 125.5, 121.9, 119.6, 116.9, 115.9, 115.5, 98.9, 68.4, 55.3, 39.8, 31.9, 29.7, 29.6, 29.5, 29.4, 26.1, 23.0, 22.7, 14.1, 13.9. λ$_{max}$(DCE)/nm 322 (ε/dm^3 mol^{-1} cm^{-1} 29933), 348 (29624) and 494 (53582). Anal. Calcd. for C$_{67}$H$_{79}$N$_3$O$_5$: C 79.96, H 7.91, N 4.18. Found: C 79.89,

H 7.93, N 4.13. MS (ESI$^+$): m/z calcd. for C$_{67}$H$_{79}$N$_3$O$_5$: 1005.6. Found 1006.2 [M+H]$^+$.

Synthesis of FBA3. A solution of dialdehyde **7** (117 mg, 0.1 mmol), cyanoacetic acid (85 mg, 1 mmol), and ammonium acetate (15 mg, 0.2 mmol) in AcOH (10 mL) was stirred under reflux for 5 h. The solvent was evaporated under reduced pressure, and the residue was taken up in DCM, washed extensively with H$_2$O, and dried over MgSO$_4$. After removal of the solvent at reduced pressure, the crude product was further purified by column chromatography (silica gel, DCM, and then DCM/AcOH 95/1). The dark paste thus obtained was washed with cold petroleum ether affording the title compound as a dark-red foam. Yield: 108 mg (82%). ^{1}H NMR (400 MHz, CDCl$_3$): δ [ppm] = 8.37 (s, 2H), 8.08 – 7.98 (m, 4H), 7.72 (d, J = 8.4 Hz, 2H), 7.62 (d, J = 8.3 Hz, 2H), 7.19 – 7.12 (m, 4H), 7.06 (dd, J = 8.4, 1.9 Hz, 2H), 6.89 (d, J = 8.9 Hz, 2H), 4.07 (t, J = 5.6 Hz, 2H), 2.48 – 2.24 (m, 2H), 2.20 – 2.09 (m, 2H), 2.06 – 1.77 (m, 8H), 1.19 – 1.05 (m, 8H), 0.73 (t, J = 7.3 Hz, 12H), 0.70 – 0.51 (m, 8H).^{13}C NMR (100.6 MHz, CDCl$_3$): δ [ppm] = 167.6, 157.0, 155.8, 154.0, 151.4, 148.8, 147.4, 140.5, 133.8, 132.0, 129.0, 127.6, 125.5, 122.1, 121.9, 119.6, 117.0, 115.9, 115.5, 99.0, 66.6, 55.3, 39.8, 27.98 (t, J_{CF} = 22 Hz), 26.1, 23.0, 20.7, 13.9. ^{19}F NMR (282 MHz, CDCl$_3$): δ [ppm] = -81.7 (t, J = 10.1 Hz, 3F), -114.3 (br s, 2F), -121.9 – -123.2 (m, 6F), -123.6 (br s, 2F), -124.3 (br s, 2F), -127.0 (br s, 2F). λ$_{max}$(DCE)/nm 318 (ε/dm^3 mol^{-1} cm^{-1} 45877), 345 (45406) and 495 (82850). Anal. Calcd. for C$_{67}$H$_{62}$F$_{17}$N$_3$O$_4$: C 61.33, H 4.76, N 3.20. Found: C 61.42, H 4.59, N 3.09. MS (ESI$^+$): m/z calcd. for C$_{67}$H$_{62}$F$_{17}$N$_3$O$_4$: 1311.4. Found 1312.2 [M+H]$^+$.
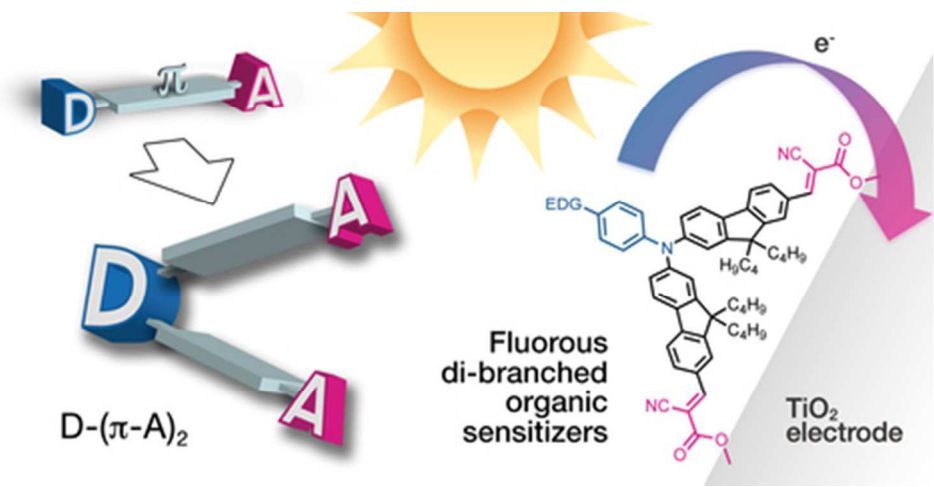
Synthesis of FBA4. A solution of dialdehyde **8** (146 mg, 0.1 mmol), cyanoacetic acid (85 mg, 1 mmol), and ammonium acetate (15 mg, 0.2 mmol) in AcOH (10 mL) was stirred under reflux for 5 h. The solvent was evaporated under reduced pressure, and the residue was taken up in Et$_2$O, washed extensively with H$_2$O, and dried over MgSO$_4$. After removal of the solvent at reduced pressure, the crude product was further purified by column chromatography (silica gel, gradient DCM to DCM/AcOH 25/1) affording the title compound as a dark-red foam. Yield: 112 mg (70%). ^{1}H NMR (400 MHz, CDCl$_3$): δ [ppm] = 8.39 (s, 2H), 8.07 – 8.01 (m, 4H), 7.75 (d, J = 8.2 Hz, 2H), 7.66 (d, J = 8.3 Hz, 2H), 7.23 – 7.14 (m, 6H), 7.08 (dd, J = 8.2, 2.0 Hz, 2H), 4.41 (s, 6H), 2.07 – 1.93 (m, 4H), 1.92 – 1.76 (m, 4H), 1.17 – 1.04 (m, 8H), 0.72 (t, J = 7.3 Hz, 12H), 0.69 – 0.58 (m, 8H).^{13}C NMR (100.6 MHz, CDCl$_3$): δ [ppm] = 167.6, 157.0, 154.2, 151.5, 148.3, 147.1, 147.0, 134.8, 131.9, 131.1, 129.3, 127.2, 125.6, 124.7, 123.2, 122.0, 120.1 (q, J_{CF} = 293 Hz), 119.8, 118.6, 115.8, 99.4, 79.4 (m), 68.0, 55.3, 48.0, 39.6, 26.1, 22.9, 13.8. ^{19}F NMR (282 MHz, CDCl$_3$): δ [ppm] = -68.7 (s). λ$_{max}$(DCE)/nm 323 (ε/dm^3 mol^{-1} cm^{-1} 47781), 351 (36187) and 482 (78920). Anal. Calcd. for C$_{72}$H$_{62}$F$_{27}$N$_3$O$_7$: C 54.24, H 3.92, N 2.64. Found: C 54.22, H 3.96, N 2.65. MS (ESI$^+$): m/z calcd. for C$_{72}$H$_{62}$F$_{27}$N$_3$O$_7$: 1593.4. Found 1593.3 [M]$^+$.

Acknowledgements

Notes and references

1 B. O'Regan and M. Grätzel, *Nature*, 1991, **353**, 737
2 A. Hagfeldt, G. Boschloo, L. C. Sun, L. Kloo and H. Pettersson, *Chem. Rev.*, 2010, **110**, 6595.
3 N. Martsinovich and A. Troisi, *Energy Environ. Sci.*, 2011, **4**, 4473.
4 E. M. J. Johansson, R. Lindblad, H. Siegbahn, A. Hagfeldt and H. Rensmo, *ChemPhysChem*, 2014, **15**, 1006.
5 B. Roose, S. Pathak and U. Steiner, *Chem. Soc. Rev.*, 2015, **44**, 8326.
6 V. S. Manthou, E. K. Pefkianakis, P. Falaras and G. C. Vougioukalakis, *ChemSusChem*, 2015, **8**, 588.
7 J. Wu, Z. Lan, J. Lin, M. Huang, F. Yunfang, L. Leqing and G. Luo, *Chem. Rev.*, 2015, **115**, 2136.
8 M. L. Parisi, S. Maranghi and R. Basosi, *Renew. Sust. Energ. Rev.*, 2014, **39**, 124.
9 A. Mishra, M. K. R. Fischer and P. Bäuerle, *Angew. Chem. Int. Ed.*, 2009, **48**, 2474.
10 J. N. Clifford, E. Martínez-Ferrero, A. Viterisi and E. Palomares, *Chem. Soc. Rev.*, 2011, **40**, 1635.
11 S. Ahmad, E. Guillen, L. Kavan, M. Grätzel and M. K. Nazeeruddin, *Energy Environ. Sci.*, 2013, **6**, 3439.
12 M. Urbani, M. Grätzel, M. K. Nazeeruddin and T. Torres, *Chem. Rev.*, 2014, **114**, 12330.
13 C.-P. Lee, R. Y.-Y. Lin, L.-Y. Lin, C.-T. Li, T.-C. Chu, S.-S. Sun, J. T. Lin and K.-C. Ho, *RSC Adv.*, 2015, **5**, 23810.
14 M. Asif, *Solar Energy*, 2016, **123**, 127.
15 W. Zeng, Y. Cao, Y. Bai, Y. Wang, Y. Shi, M. Zhang, F. Wang, C. Pan and P. Wang, *Chem. Mater.*, 2010, **22**, 1915.
16 Y. Xie, Y. Tang, W. Wu, Y. Wang, J. Liu, X. Li, H. Tian and W.-H. Zhu, *J. Am. Chem. Soc.*, 2015, **137**, 14055.
17 Z.-S. Huang, H. Meier and D. Cao, *J. Mater. Chem. C*, 2016, **4**, 2404.
18 A. Abbotto, N. Manfredi, C. Marinzi, F. De Angelis, E. Mosconi, J.-H. Yum, Z. Xianxi, M. K. Nazeeruddin and M. Grätzel, *Energy Environ. Sci.*, 2009, **2**, 1094.
19 N. Manfredi, B. Cecconi and A. Abbotto, *Eur. J. Org. Chem.*, 2014, **32**, 7069.
20 X.-X. Dai, H.-L. Feng, Z.-S. Huang, M.-J. Wang, L. Wang, D.-B. Kuang, H. Meier and D. Cao, *Dyes Pigments*, 2015, **114**, 47.
21 D. Heredia, J. Natera, M. Gervaldo, L. Otero, F. Fungo, C.-Y. Lin and K.-T. Wong, *Org. Lett.*, 2010, **12**, 12.
22 L. Macor, M. Gervaldo, F. Fungo, L. Otero, T. Dittrich, C.-Y. Lin, L.-C. Chi, F.-C. Fang, S.-W. Lii, K.-T. Wong, C.-H. Tsai and C.-C. Wu, *RSC Adv.*, 2012, **2**, 4869.
23 G. Pozzi, S. Orlandi, M. Cavazzini, D. Minudri, L. Macor, L. Otero and F. Fungo, *Org. Lett.*, 2013, **15**, 4642.
24 A. Baheti, P. Tyagi, K. R. Justin Thomas, Y.-C. Hsu and J. T. Lin, *J. Phys. Chem. C*, 2009, **113**, 8541.
25 L.-Y. Lin, C.-H. Tsai, K.-T. Wong, T.-W. Huang, C.-C. Wu, S.-H. Chou, F. Lin, S.-H. Chen and A.-I. Tsai, *J. Mater. Chem.*, 2011, **21**, 5950.
26 G. Marzari, J. Durantini, D. Minudri, M. Gervaldo, L. Otero, F. Fungo, G. Pozzi, M. Cavazzini, S. Orlandi and S. Quici, *J. Phys. Chem. C*, 2012, **116**, 21190.
27 F. Zhang, W. Ma, Y. Jiao, J. Wang, X. Shan, H. Li, X. Lu and S. Meng, *ACS Appl. Mater. Interfaces*, 2014, **6**, 22359.
28 S. Sarker, H. W. Seo, Y.-K. Jina, K.-S. Lee, M. Lee and D. M. Kim, *Electrochim. Acta*, 2015, **182**, 493.
29 F. Wu, X. Li, Y. Tong and T. Zhang, *J. Power Sources*, 2017, 342 704.
30 Z.-S. Wang, H. Kawauchi, T. Kashima and H. Arakawa, *Coord. Chem. Rev.*, 2004, **248**, 1381.
31 W. Li, Y. Wu, X. Li, Y. Xie and W. Zhu, *Energy Environ. Sci.*, 2011, **4**, 1830.
32 F. Bella, G. Leftheriotis, G. Griffini, G. Syrrokostas, S. Turri, M. Grätzel and C. Gerbaldi, *Adv. Funct. Mat.*, 2016, **26**, 1127.
33 A.-L. Anderson, S. Chen, L. Romero, I. Top and R. Binions, *Buildings*, 2016, **6**, 37.
34 M. J. Xiong, H. L. Zhong and M. S. Wong, *Aust. J. Chem.*, 2007, **60**, 608.
35 C. M. Cardona, W. Li, A. E. Kaifer, D. Stockdale and G. C. Bazan, *Adv. Mater.*, 2011, **23**, 2367.

39x19mm (300 x 300 DPI)